

# A Magnesium-Incorporated Nanoporous Titanium Coating for Rapid Osseointegration

This article was published in the following Dove Press journal:  
*International Journal of Nanomedicine*

Xiaodong Li,<sup>1</sup> <sup>1-3,\*</sup>  
Mingyi Wang,<sup>3,\*</sup> Wenjie Zhang,<sup>4</sup>  
Yuting Bai,<sup>2</sup> Yuan Liu,<sup>3</sup>  
Jian Meng,<sup>1,2</sup> Ling Zhang<sup>3</sup>

<sup>1</sup>School of Stomatology, Weifang Medical University, Weifang, Shandong Province, People's Republic of China; <sup>2</sup>Department of Stomatology, Central Hospital of Xuzhou, The Xuzhou Clinical College of Xuzhou Medical University, Xuzhou, Jiangsu Province, People's Republic of China;

<sup>3</sup>Department of Oral Maxillofacial-Head and Neck Oncology, Shanghai Ninth People's Hospital, College of Stomatology, Shanghai Jiao Tong University School of Medicine, National Clinical Research Center for Oral Diseases, Shanghai Key Laboratory of Stomatology & Shanghai Research Institute of Stomatology, Shanghai, People's Republic of China;

<sup>4</sup>Department of Prosthodontics, Oral Bioengineering and Regenerative Medicine Lab, Ninth People's Hospital Affiliated to Shanghai Jiao Tong University, School of Medicine, Shanghai, People's Republic of China

\*These authors contributed equally to this work

Correspondence: Jian Meng  
Department of Stomatology, Central Hospital of Xuzhou, The Xuzhou Clinical College of Xuzhou Medical University, Xuzhou, Jiangsu Province 221000, People's Republic of China  
Tel +86 18952170986  
Email mrocket@126.com

Ling Zhang  
Department of Oral Maxillofacial-Head and Neck Oncology, Shanghai Ninth People's Hospital, College of Stomatology, Shanghai Jiao Tong University School of Medicine, National Clinical Research Center for Oral Diseases, Shanghai Key Laboratory of Stomatology & Shanghai Research Institute of Stomatology, Shanghai 200011, People's Republic of China  
Tel +86 18019791107  
Email topgun1128@163.com

**Purpose:** Micro-arc oxidation (MAO) is a fast and effective method to prepare nanoporous coatings with high biological activity and bonding strength. Simple micro/nano-coatings cannot fully meet the requirements of osteogenesis. To further improve the biological activity of a titanium surface, we successfully added biological magnesium ( $Mg^{2+}$ ) to a coating by micro-arc oxidation and evaluated the optimal magnesium concentration in the electrolyte, biocompatibility, cell adhesion, proliferation, and osteogenesis in vitro.

**Methods:** Nanoporous titanium coatings with different concentrations of magnesium were prepared by micro-arc oxidation and characterized by scanning electron microscopy (SEM) and energy-dispersive X-ray spectroscopy (EDS). The  $Mg^{2+}$  release ability of the magnesium-incorporated nanoporous titanium coatings was determined by inductively coupled plasma emission spectrometry (ICP-OES). The cytotoxicity of the magnesium-incorporated nanoporous titanium coatings was detected with live/dead double-staining tests. A CCK-8 assay was employed to evaluate cell proliferation, and FITC-phalloidin was used to determine the structure of the cytoskeleton by staining  $\beta$ -actin. Alkaline phosphatase (ALP) activity was evaluated by alizarin red S (ARS) staining to determine the effect of the coatings on osteogenic differentiation in vitro. The mRNA expression of osteogenic differentiation-related markers was measured using qRT-PCR.

**Results:** EDS analyses revealed the successful addition of magnesium to the microporous coatings. The best magnesium concentration of the electrolyte for preparing the new coating was determined. The results showed that the nano-coatings prepared using the electrolyte with 2 g/L magnesium acetate best promoted the adhesion, proliferation, and osteogenic differentiation of bone marrow mesenchymal stem cells (BMSCs).

**Conclusion:** These results suggest that the new titanium metal coating with a dual effect of promoting bone morphology and supplying the biological ion  $Mg^{2+}$  can be beneficial for rapid osseointegration.

**Keywords:** micro/arc oxidation, magnesium-incorporated nanoporous coating, osteoinductivity

## Introduction

In addition to excellent deformation properties and fatigue resistance, titanium is nontoxic, noncarcinogenic, and biocompatible, allowing it to be widely used in the medical field. Since Professor Brånemark proposed the theory of osseointegration, titanium has been introduced into the field of dental restorations.<sup>1</sup> However, titanium-based implant materials have limitations, including limited osteoinductive capability and high elastic modulus. At least 3 months after titanium-based implants are implanted, adequate osseointegrated fixation can be obtained.<sup>2</sup> Titanium is a biologically inert material,<sup>3</sup> and due to its poor surface bone conductivity, it

cannot be sufficiently osseointegrated. Owing to these shortcomings, the interface between bone tissue and titanium is not strong enough to achieve a mechanical seal and fixation, and it takes a long time to stabilize.

To improve the surface activity of titanium implants and strengthen the binding ability of materials and bone tissue, various modifications have been added to the surface of titanium implants.<sup>4</sup> Micro-arc oxidation (MAO)<sup>5</sup> uses the combination of an electrolyte and corresponding electrical parameters to grow in situ ceramic coatings mainly composed of substrate metal oxides on the surfaces of metals, such as aluminum, magnesium, titanium, and their alloys, via the instantaneous high temperature and high pressure that are generated by an arc discharge. Ceramic coatings have been widely used in the surface modification of titanium and its alloys.<sup>6–8</sup> MAO can allow the surface of titanium to form a microporous structure, letting cells better adhere to the material surface and fully stimulating bone formation. Nanostructured surfaces can directly interact with certain proteins and cell membrane receptors, effectively enhancing cell function. Micro/nano-structures have a certain positive effect on osteogenesis.<sup>7</sup> MAO can not only change the surface morphology of the metal substrate but also add various nutritional elements, such as copper, silver, zinc, strontium, and silicon, depending on the characteristics of its electrolyte.<sup>9–12</sup> The addition of these chemical elements changes the biological properties of the material and improves the antibacterial, adhesion, and osteogenic activities.

Magnesium is an important component of bone tissue. The concentration of  $Mg^{2+}$  ranks fourth among all cations in the human body. More than half of the magnesium in the human body is stored in bone tissue in the form of biological magnesium.<sup>13</sup>  $Mg^{2+}$  are the most abundant divalent cations in cells, regulating multiple cellular functions, including cell signaling, cell growth, metabolism, and proliferation. High concentrations of magnesium ions can activate calcium ion channels on cell membranes<sup>14</sup> and promote calcium deposition, and magnesium is required for bone growth.

In this study, MAO was used to prepare magnesium-containing nano-coatings on a titanium surface. In this coating, the advantages of the two metals, Mg and Ti, are complementary. The dual effect of the nanostructure of the coating and the release of Mg ions induce bone formation. By the addition of magnesium, the coating not only retains the excellent mechanical properties of titanium but also possesses the enhanced biological activities

of titanium. We further determined the optimal electrolyte concentration in the preparation of magnesium-containing nano-coatings, and observed the activity, adhesion, and osteogenic differentiation of osteoblasts on the magnesium-containing nano-coatings to determine whether the material can be applied in clinical practice.

## Materials and Methods

### Fabrication and Characterization of MAO-Mg Coating

The titanium sheets ( $20 \times 20 \times 1$  mm and  $10 \times 10 \times 1$  mm) used in the experiment were cut from commercial TC4 titanium alloy. The cut sample was sequentially cleaned in acetone, ethanol, and distilled water in an ultrasonic cleaner.

Then, the samples were micro-arc-oxidized in an electrolyte solution composed of 17.6 g/L calcium acetate monohydrate ( $Ca(CH_3COO)_2 \cdot H_2O$ , Sinopharm, Shanghai, China) and 4.74 g/L sodium phosphate dibasic dihydrate ( $NaH_2PO_4 \cdot 2H_2O$ , Sinopharm, Shanghai, China) to fabricate a porous surface layer (the MAO coating). The voltage, frequency and time parameters of the pulsed AC power were 420 V, 50 Hz, and 10 min, respectively. To load magnesium into the porous surface layer (the MAO-Mg coating), magnesium acetate ( $C_4H_6MgO_4 \cdot 4H_2O$ , Sinopharm, Shanghai, China, 1 g/L, 2 g/L, 4 g/L, 8 g/L) was added to the electrolyte. The MAO microporous coatings incorporated with different amounts of  $Mg^{2+}$  were named M1, M2, M4, and M8, respectively.

### Material Characteristics

Scanning electron microscopy (SEM, JEOL, Japan) was used to scan the surface morphology of the samples, and the coating roughness was measured by the Perthometer M1 (Marl, Germany) measuring instrument. Then, ImageJ software (National Institutes of Health, USA) was used to analyze the distribution of pore sizes of the coatings. The wettability of the coating surface was determined using a contact angle meter (SL200B, Solon, China). The elemental composition of the samples was determined by energy-dispersive X-ray spectroscopy (EDS, EPMA, Japan).

### Magnesium Ion Release

The samples were immersed in 4mL of standard phosphate buffer saline (PBS) and then incubated at 37°C under gentle shaking. The  $Mg^{2+}$  concentration of the buffer solution at different time points (1, 4 and 7 days) was

measured by inductively coupled plasma/optical emission spectroscopy (ICP-OES, Varian, USA).

## Culture of Murine BMSCs

Four-week-old Sprague–Dawley (SD) rats provided by the Central Laboratory of Shanghai Ninth People's Hospital were used to collect bone marrow mesenchymal stem cells (BMSCs). The rats were sacrificed by spinal dislocation and placed in 75% alcohol for 3 min. The tibia and femur were removed, and the bone marrow cavity was washed with Dulbecco's Modified Eagle's Medium (DMEM) medium containing 1% penicillin-streptomycin (Thermo Fisher Scientific, USA) and 10% fetal bovine serum (FBS, Gibco, USA). The collected bone marrow washings were centrifuged at 1000 rpm for 10 min. Cells were cultivated in DMEM in an incubator at 37°C with 5% CO<sub>2</sub>. After 5 days of cultivation, nonadherent cells were removed, and fresh medium was added. The remaining adherent cells were mainly BMSCs. Subculture was conducted when the cells reached 80–90% confluence. BMSCs at passage 2 to 4 with strong growth activity were used as the experimental cells.

## Cell Activity and Proliferation Experiment

BMSCs were seeded on samples of the six groups. Twenty-four hours later, to assess cell viability on the different substrates, the Calcein-AM/PI Double Stain Kit (Yeasen, Shanghai, China) was applied. Cell adhesion and proliferation were evaluated by the Cell Counting Kit-8 (CCK-8, Beyotime, Shanghai, China). The density of the cell suspension was  $2 \times 10^4$  cells/mL. Cells were incubated with the different metal samples (10×10×1 mm) for 1 day, 3 days and 7 days at 37°C, 5% CO<sub>2</sub>. At the required time point, Samples were washed three times by PBS. Then, 500 μL of serum-free medium and 50 μL of CCK-8 mixed reagent were added to each well, and the plate was incubated for 1.5 h. Next, 100 μL/well supernatant was pipetted to 96-well plates. The optical density of the culture was determined by spectrophotometry in a microplate reader. To observe the cell coverage area, FITC-phalloidin (Enzo Life Science Ltd, Exeter, UK) was used to determine the structure of the cytoskeleton by staining β-actin.

The cells were seeded on samples for 6 h, then fixed with 4% paraformaldehyde (Sigma, St Louis, MO, USA) and permeabilized with 0.5% Triton X-100 (Sigma). The cytoskeleton and nuclei were stained with phalloidin and DAPI (Invitrogen, Carlsbad, CA, USA), respectively. The extension area of cells was measured by ImageJ. Cell fluorescence area is expressed as total area/cell number.

## ALP Activity and Calcium Deposition

BMSCs were fixed and stained with an ALP kit (Beyotime, Shanghai, China) after culture in DMEM for 7 days. At the same time, the ALP was quantitatively analyzed by p-nitrophenyl phosphate (pNPP) (Sigma). The ALP activity is presented as optical density (OD) value at 405 nm per milligram of total protein. After culture in DMEM for 7 days, calcium deposition assays were further performed. First, the cells were fixed with 70% ethanol and stained by 40 mM alizarin red S (ARS, Sigma) solution. Then, the staining “hole” was eluted with 10% cetylpyridinium chloride (Sigma) solution, and OD values were measured at 590 nm for quantitative analysis. The results of calcium deposition were normalized by total protein content and are expressed as OD value at 590 nm per milligram of total protein in the cells.

## Expression of Osteogenic-Related Genes

BMSCs were cultured on substrates for 7 days, and total RNA was extracted with TRIzol reagent (Invitrogen, Thermo Fisher Scientific, USA). cDNAs were synthesized using a PrimeScript 1-strand cDNA synthesis kit (Takara, Japan). The expression of osteogenic genes *Runt-related transcription factor 2 (Runx2)*, *ALP* and *OCN* was detected by qRT-PCR (Bio-Rad, MyiQ, USA). The housekeeping gene *glyceraldehyde-3-phosphate dehydrogenase (GAPDH)* was used for standardization. The primers are listed in Table 1.<sup>5</sup>

## Statistical Analysis

All the data are presented as the mean ± standard deviation (SD). The data were analyzed using GraphPad Prism (GraphPad Software, USA). One-way ANOVA followed

**Table 1** Primers for qRT-PCR

Gene Prime	Forward Primer	Reverse Primer	Product Length	Accession
ALP	ACCGCAGGATGTGAACTACT	GAAGCTGTGGGTTCACTGGT	90	XM_006253120.2
OCN	ATTGTGACGAGCTAGCGGAC	GCAACACATGCCCTAAACGG	83	NC_005101.4
Runx2	CCTTCCCTCCGAGACCCTAA	ATGGCTGCTCCCTTCTGAAC	90	NM_001278484.2
GAPDH	CAGGGCTGCCTTCTTTGTG	AACTTGCCGTGGGTAGAGTC	111	NM_017008.4

by the Tukey's post hoc test was used to determine the level of significance.  $p < 0.05$  was considered significant.

## Results

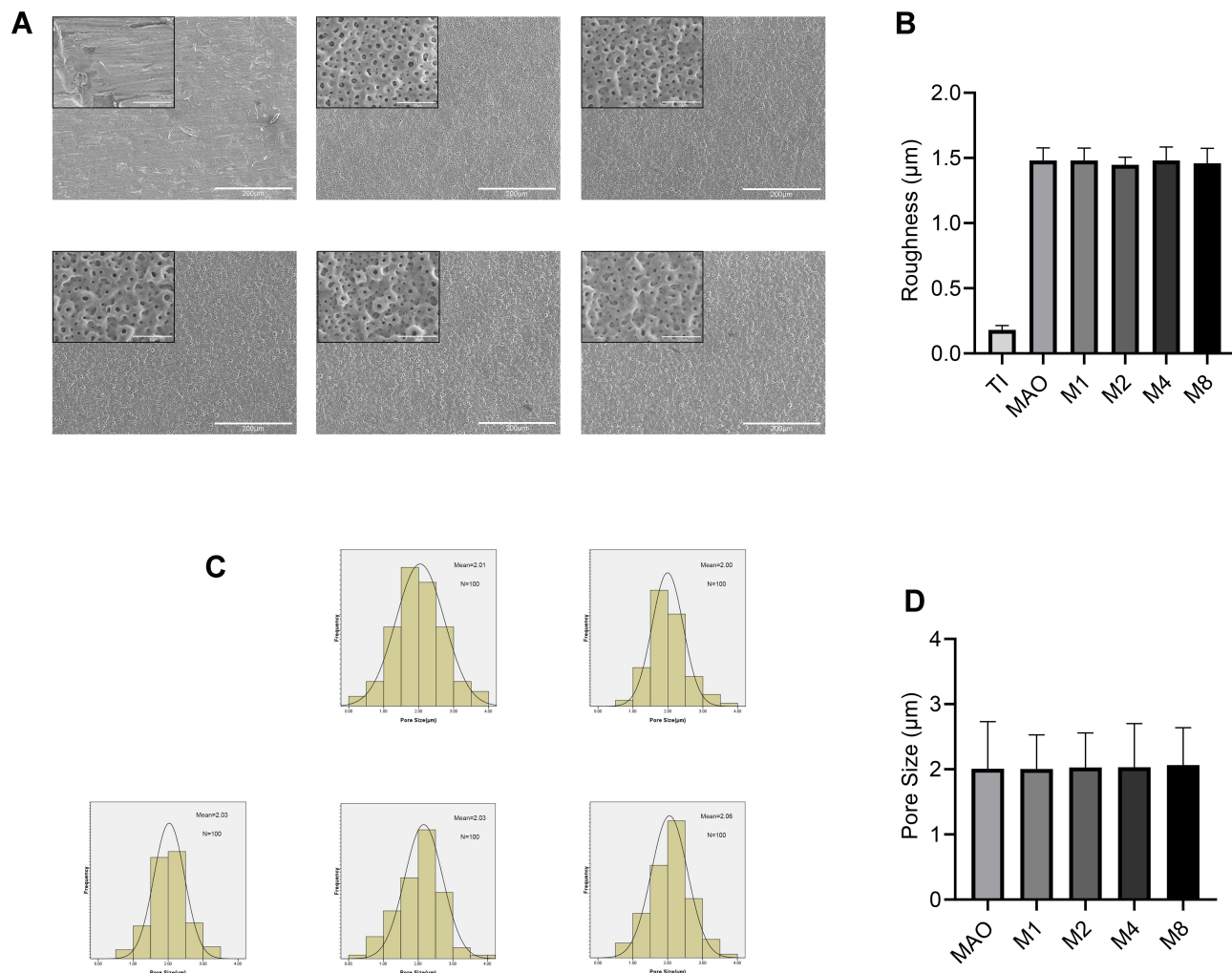
### Surface Morphology

Figure 1A shows the surface morphology of all groups. Compared with the Ti group, other coatings had similar microporous structures without significant differences. Figure 1C shows the frequency distribution of the pore size. The minimum pore size and maximum pore size were  $0.34 \mu\text{m}$  and  $4.2 \mu\text{m}$ , respectively, and the average was  $2.01 \mu\text{m}$ . Compared with the MAO group, there was no significant difference in the pore size of the coating with magnesium (Figure 1D). The roughness results (Figure 1B) showed that the surface roughness of the MAO-treated groups (MAO, M1, M2, M4, M8) was

significantly higher than that of Ti, but there was no significant difference among the MAO-treated groups. As shown in Figure 2, compared with the Ti group, the surfaces of MAO-treated groups exhibited larger contact angles, but no significant difference was observed among the MAO-treated groups.

We analyzed the element composition of the material surface by EDS (Figure 3) and found that the  $\text{Mg}^{2+}$  was successfully incorporated into the microporous coating. The  $\text{Mg}^{2+}$  content in the coating could be controlled by adjusting the magnesium acetate concentration. As the concentration of magnesium acetate increased, the concentration of  $\text{Mg}^{2+}$  in the coating increased (Figure 3).

As shown in Figure 4, Magnesium ions were successfully released from the material into the solution from magnesium-incorporated coatings and the concentration



**Figure 1** (A) SEM images of six sample surfaces. (B) The roughness of the five coatings (C) The frequency distribution of the pore size. (D) The pore size of the five coatings.

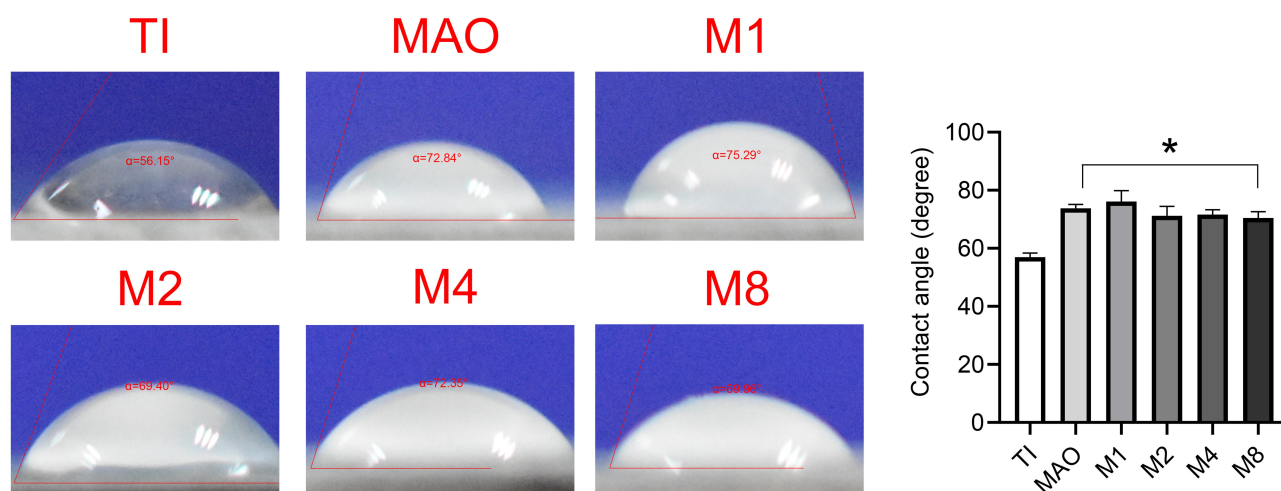


**Figure 2** The contact angle of the six sample (\* $p < 0.05$  compared with Ti).

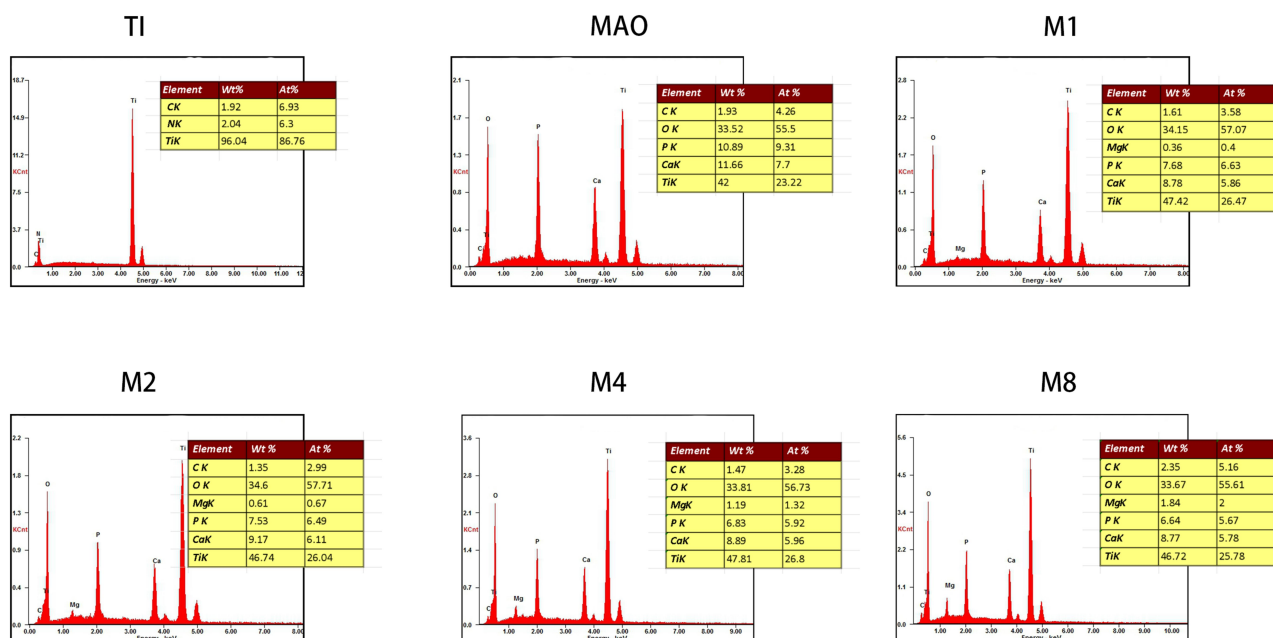


**Figure 3** EDS and elemental analysis of the six sample.

of  $Mg^{2+}$  in solution increased with the increasing of magnesium content in the material.

## Cell Cytotoxicity and Proliferation

**Figure 5A** presents images of the live/dead staining of cells on the all samples. Almost all cells were alive in the Ti, MAO, M1, M2, M4, and M8 groups. Compared to the Ti group, there was no significant decrease in the number of living (green) cells in the M1, M2, M4, or M8 group. While sporadic dead cells (red) were present on the all surfaces, there was no obvious increase in the number of dead cells in the M1, M2, M4, and M8 groups. The statistical results

showed that all groups were similar (**Figure 5B**), which confirmed that  $Mg^{2+}$  had no lethal toxicity to cell growth.

The result of the cell proliferation test (**Figure 5C**) showed that the low-concentration  $Mg^{2+}$  layer performed significantly better than Ti alone and MAO. As  $Mg^{2+}$  quantity increased, a trend of first rising and then falling was seen. As cell culture time went on, the MAO, M1, M2, and M4 groups promoted cell proliferation. The optimal concentration for cell proliferation was M2 (magnesium acetate in the electrolyte at 2 g/L).

The coverage area of BMSCs was observed after incubating on the titanium plates for 6 h (**Figure 5D**). More

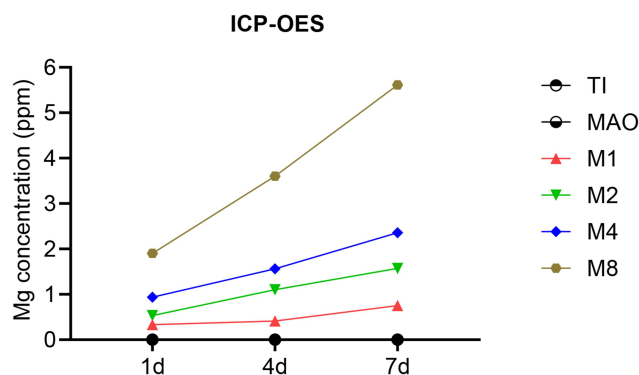


**Figure 4** ICP detection of magnesium ion release from various coatings.

BMSCs adhered to the surface of the M2 group during the initial 6 h. As shown in [Figure 5D](#), actin protein expression was clearly observed in the osteoblasts in all groups. Compared with the other groups, cytoskeleton staining on the surface of the M2 materials showed better extension ([Figure 5E](#)).

## ALP Activity and Calcium Deposition

In the ALP activity assay, the low-concentration magnesium coatings (M1 and M2 groups) showed deeper ALP staining than other groups. Moreover, the M2 group showed the best results ([Figure 6A](#)). ALP quantitative results indicated that the M2 group had significantly more ALP than the other groups ([Figure 6B](#)). Similar results were observed by alizarin red S staining and quantitative calculation via the calcium deposition assay ([Figure 6C](#) and [D](#)). All of the above results indicated that as the magnesium ion concentration in the coating increased, the osteogenesis showed a trend of first increasing and then decreasing, and the M2 group had the best effect on osteogenic differentiation of BMSCs.

## Expression of Osteogenic-Related Genes

Runx2 is a key transcription factor in osteoblast differentiation, qRT-PCR showed that M2 had significantly higher Runx2 mRNA expression than the Ti, MAO, M1, M4, and M8 groups ([Figure 7A](#)). As shown in [Figure 7B](#), the expression level of ALP in the M2 group was significantly higher than that in the Ti, MAO, M4 and M8 groups. M1 group and M2 group showed an upward trend compared with the M4, and M8 groups, while the M2 group showed the highest upward trend. OCN quantification ([Figure 7C](#)) indicated that the M2 group and M1 group had significantly more than the control group. Moreover, the OCN expression level in the M2 group was higher than

that in the other groups. The above results indicate that the magnesium-incorporated nanoporous titanium coating (M2) was most beneficial to osteoblasts.

## Discussion

To improve the biological and mechanical properties of titanium implants, many studies have been conducted on the modification of titanium and titanium metal surfaces. The surface modification of materials mainly involves modifying its surface morphology<sup>15,16</sup> and chemical composition.<sup>4,17</sup> There are various methods for generating micro-scale morphological features of titanium implant materials, such as machining, acid etching, sandblasting, plasma spraying, and MAO.<sup>18,19</sup> MAO can produce a micro- or nano-porous coating to build a cellular micro-environment with pore size on the nano-, sub-micro-, and micro-scales. The multiscale porous structure can provide the necessary space and environment for the growth of different cells and tissues, promote the formation of extracellular matrix, the transport of nutrients, and the growth of nerves and blood vessels.<sup>20</sup> The coating is considered to be a bionic coating that can effectively increase the biocompatibility of the alloy substrate, reduce the rejection generated by the body, and allow the osteoblasts to proliferate more easily and adhere to the surface of the material.<sup>21</sup>

The simple microporous nano-morphology cannot fully meet the needs of osteogenesis. The addition of biological elements (specifically, ions) gives the material better biological properties.  $Mg^{2+}$  ions are abundant in cells.  $Mg^{2+}$  participates in various biological mechanisms, such as regulation of ion channels, DNA stabilization, enzyme activation, and cell growth, metabolism, and proliferation.<sup>13,14</sup>  $Mg^{2+}$  ions can promote the expression of integrin in human osteoblasts and enhance the adhesion of osteoblasts.<sup>22</sup> Magnesium-containing implants can promote osteoblast maturation.<sup>23,24</sup>

MAO can deposit the bioactive elements in an electrolyte onto the surface of titanium implants. After an appropriate amount of magnesium acetate is added to the electrolytic solution, the magnesium acetate can be dissolved in water and form a clear and uniform solution without turbidity. In this study, the EDS scan found that the proportion of magnesium on titanium sheets increased with increasing magnesium concentration in the electrolyte, and the ion distribution on the surface of the material could be adjusted by adjusting the ion concentration in the electrolyte.<sup>25</sup> The SEM images revealed that the addition

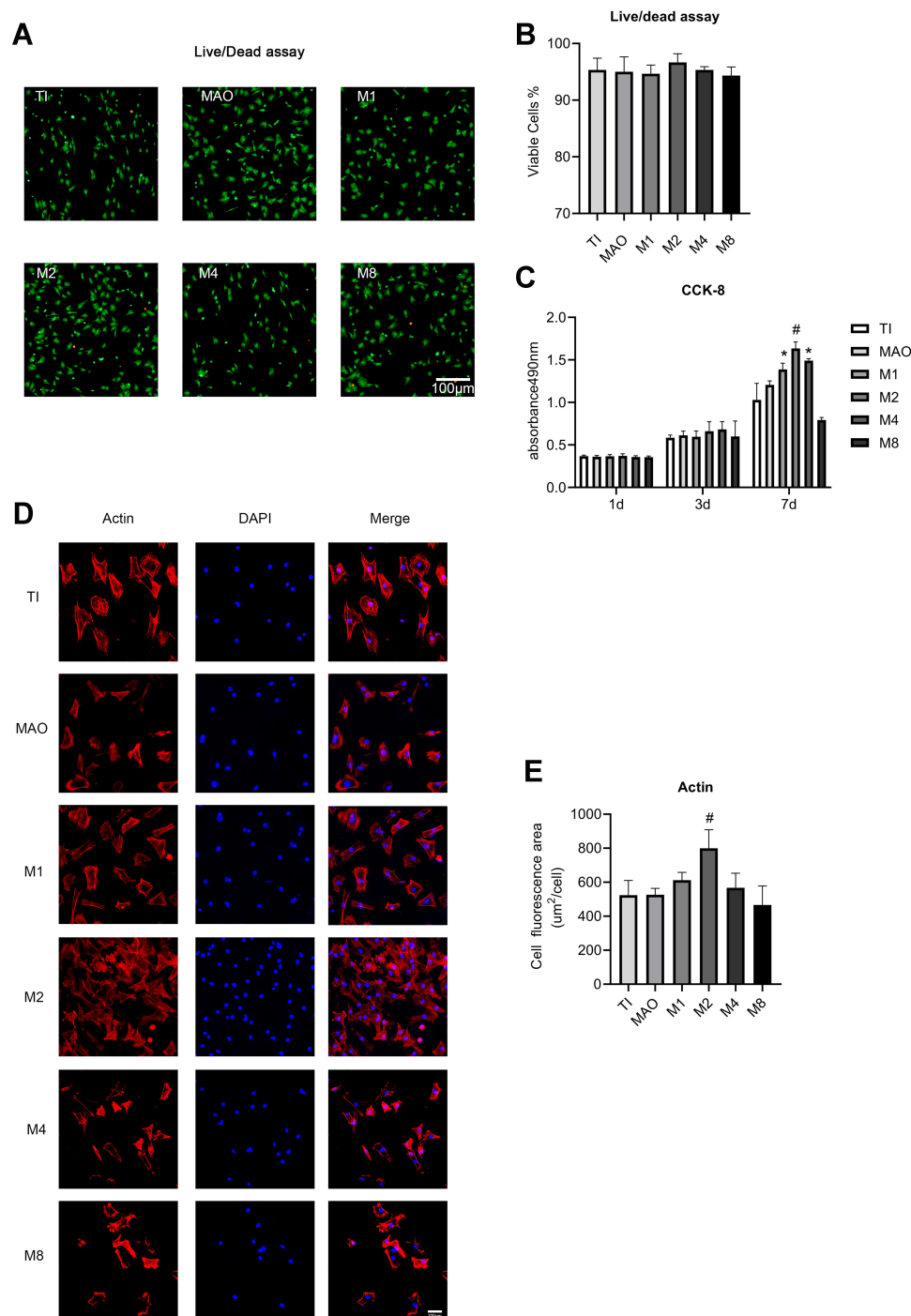


**Figure 5** (A) Live/dead assay of cells cultured for 24 h on the samples. Scale bar = 100 µm. (B) Statistical results of the live/dead assay. (C) Cell proliferation measured by CCK-8 assay after 1, 3, and 7 days of culture. (D) Fluorescence images of actin (red) and nuclei (blue) in cells cultured on the samples for 6 h. Scale bar = 100 µm. (E) The average area of cell actin was determined by ImageJ (\* $p < 0.05$  compared with TI and MAO; # $p < 0.05$  compared with TI, MAO, M1, M4, and M8).

of  $Mg^{2+}$  ions did not destroy the microporous morphology formed by MAO. The roughness and contact angle of the material do not change with the increasing of magnesium. The addition of magnesium ions simply changed the ion distribution on the coating surface, in line with the results of other studies.<sup>12</sup> In this study, the magnesium-containing

microporous coatings prepared by MAO not only had micro/nano-pores but also released  $Mg^{2+}$  ions to form a local high-magnesium microenvironment for cell growth (Figure 4).

The successful addition of magnesium to the coating lays the foundation for later research; a higher magnesium

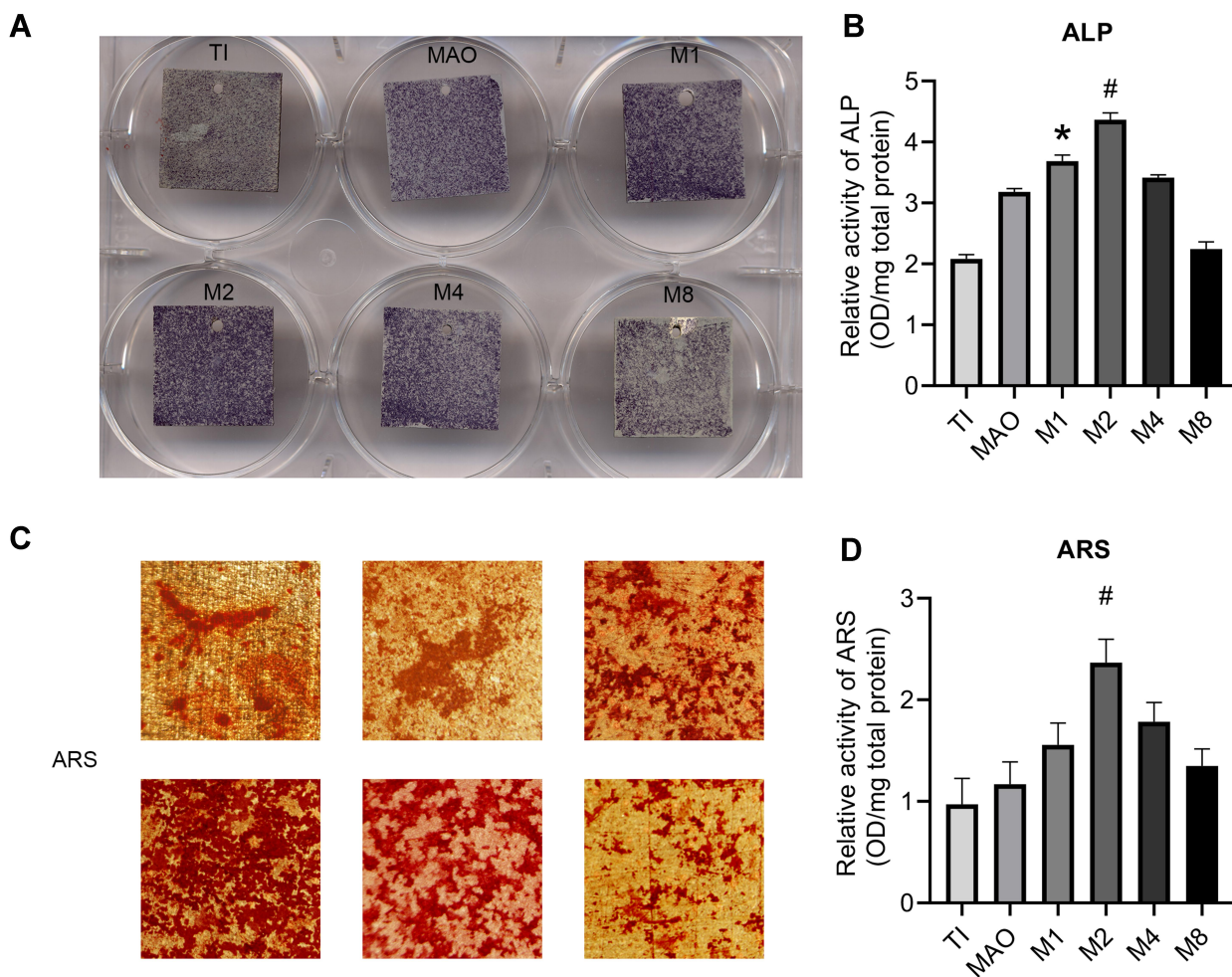


**Figure 6** ALP activity and calcium deposition. **(A)** After 7 days of culture, BMSCs on the different coatings were stained with ALP. **(B)** ALP activity was measured using a quantitative colorimetric assay. **(C)** After 21 days of culture, BMSCs on the different coatings were stained with ARS. **(D)** Calcium deposition activity was assayed using a quantitative colorimetric assay (\* $p < 0.05$  compared with Ti and MAO; # $p < 0.05$  compared with Ti, MAO, M1, M4, and M8).

content on the titanium surface does not lead straight to a better result. We studied various concentrations of  $Mg^{2+}$ , and adhesion and proliferation experiments showed that with the increase in the  $Mg^{2+}$  concentration on the material surface, the biological properties of the material showed a downward trend after an initial increase. High concentration of  $Mg^{2+}$  was not favorable for cell adhesion and proliferation. The intermediate-concentration coating (M2 group) provided the best result. As the  $Mg^{2+}$  ions released by the material form a biological microenvironment suitable for cell growth, the concentration of  $Mg^{2+}$  ions affects the substrate proteins and transcription factors, thus increasing the osteogenic effect.<sup>26</sup> The microenvironment formed by  $Mg^{2+}$  ions also has certain concentration requirements: it is difficult to achieve the osteogenic effect at a low concentration, and a high concentration is not

favorable for cell growth.<sup>27</sup> An appropriate  $Mg^{2+}$  concentration is critical for the application of the material. We found that although high magnesium was not toxic to the cells, it affected the overall cell proliferation. Because magnesium is easily degraded, a high  $Mg^{2+}$  concentration around the material affects the pH and is not favorable for the growth of osteoblasts.<sup>28,29</sup> The results of ALP staining and calcium deposition revealed that the optimal magnesium-containing coating (M2 group) also showed a good osteogenesis trend, significantly better than in other groups. In summary, an appropriate  $Mg^{2+}$  concentration can not only promote the adhesion and proliferation of osteoblasts but also accelerate their osteogenic differentiation.

Runx2 is a key transcription factor for osteoblast differentiation and plays a role in the early stage of new bone



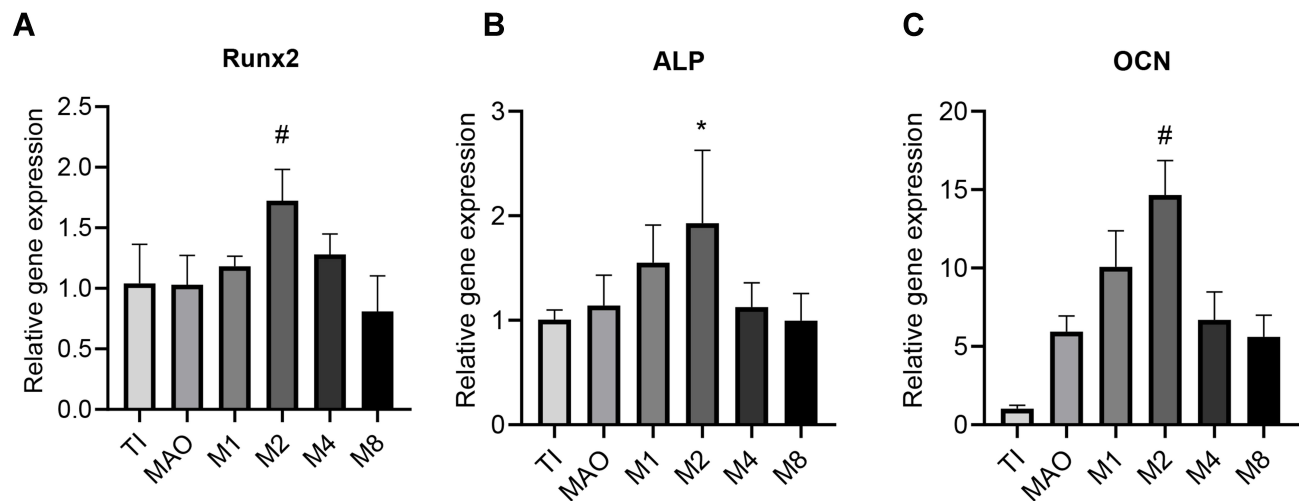


**Figure 7** Expression of osteogenic-related genes was measured by qRT-PCR after incubating on different coatings for 7 days (n=3). (A) Runx2 expression. (B) ALP expression. (C) OCN expression (\*p<0.05 compared with Ti and MAO; #p<0.05 compared with Ti, MAO, M1, M4, and M8).

formation.<sup>30,31</sup> ALP is an important marker of pre-osteogenic differentiation and osteogenic mineralization.<sup>32</sup> Osteocalcin (OCN) appears in the late period, and OCN is an important gene in the process of mineral deposition and is expressed in the late stage of osteogenesis.<sup>32,33</sup> qRT-PCR results also showed that the expression of Runx2, ALP, and OCN genes in the magnesium-containing porous nano-coatings (M2) were higher than those in the pure MAO group (MAO) and pure titanium group (Ti). This finding demonstrates that a magnesium-containing coating can promote BMSC differentiation into bone in the early, middle, and late stages of osteogenesis by both physical-morphological and chemical modifications.

## Conclusions

The new magnesium-containing nano-coating prepared in this study was successfully doped with magnesium, and the optimal concentration of magnesium acetate in the MAO electrolyte was 2 g/L. The magnesium-containing porous micro/nano-coating was beneficial to the adhesion, proliferation, and osteogenic differentiation of BMSCs. These results suggest that a new titanium metal coating with a dual effect of promoting bone morphology and providing the biological ion Mg<sup>2+</sup> can be beneficial for rapid osseointegration.

## Abbreviations

MAO, Micro-arc oxidation; SEM, Scanning electron microscope; EDS, Energy-dispersive X-ray spectroscopy; ICP-OES, Inductively coupled plasma; ALP, Alkaline

phosphatase; ARS, Alizarin red S; BMSCs, Bone marrow mesenchymal stem cells; PBS, Phosphate buffer saline; CCK-8, The Cell Counting Kit-8.

## Data Sharing Statement

The datasets used and/or analyzed during the current study are available from the two corresponding authors upon reasonable request.

## Ethics Approval and Informed Consent

The study was approved by the Institutional Animal Care and Use Committee of Ninth People's Hospital Affiliated to Shanghai Jiao Tong University (reference no. SH9H-2020-A116-1). All animals were followed by the guidelines of the National Institutes of Health guide for the care and use of laboratory animals (NIH Publications No. 8023, revised 1978).

## Funding

This work was supported by the National Natural Science Foundation of China (No. 81771127), the Xuzhou Medical Innovation and Technological Breakthrough Team Project (XWCX201604), the Jiangsu Health and Family Planning Commission Project of Scientific Research (H2017080), and the Xuzhou Science and Technology Project (KC17196).

## Disclosure

The authors report no conflicts of interest in this work.

## References

- Branemark PI, Adell R, Breine U, Hansson BO, Lindstrom J, Ohlsson A. Intra-osseous anchorage of dental prostheses: I. Experimental studies. *Scand J Plast Reconstr Surg.* 1969;3(2):81–100. doi:10.3109/02844316909036699
- Albrektsson T, Zarb G, Worthington P, Eriksson AR. The long-term efficacy of currently used dental implants: a review and proposed criteria of success. *Int J Oral Maxillofac Implants.* 1986;1(1):11–25.
- Geetha M, Singh AK, Asokamani R, Gogia AK. Ti based biomaterials, the ultimate choice for orthopaedic implants – a review. *Prog Mater Sci.* 2009;54(3):397–425. doi:10.1016/j.pmatsci.2008.06.004
- Zhang W, Cao H, Zhang X, et al. A strontium-incorporated nanoporous titanium implant surface for rapid osseointegration. *Nanoscale.* 2016;8(9):5291–5301. doi:10.1039/C5NR08580B
- Zhou W, Huang O, Gan Y, Li Q, Zhou T, Xi W. Effect of titanium implants with coatings of different pore sizes on adhesion and osteogenic differentiation of BMSCs. *Artif Cells Nanomed Biotechnol.* 2019;47(1):290–299. doi:10.1080/21691401.2018.1553784
- Khanna R, Kokubo T, Matsushita T, et al. Novel artificial hip joint: a layer of alumina on Ti-6Al-4V alloy formed by micro-arc oxidation. *Mater Sci Eng C Mater Biol Appl.* 2015;55:393–400. doi:10.1016/j.msec.2015.05.021
- Pan X, Li Y, Abdullah AO, Wang W, Qi M, Liu Y. Micro/nano-hierarchical structured TiO<sub>2</sub> coating on titanium by micro-arc oxidation enhances osteoblast adhesion and differentiation. *R Soc Open Sci.* 2019;6(4):182031. doi:10.1098/rsos.182031
- Xu L, Li J, Xu X, et al. A novel cytocompatibility strengthening strategy of ultrafine-grained pure titanium. *ACS Appl Mater Interfaces.* 2019;11(51):47680–47694. doi:10.1021/acsami.9b13554
- Huang Q, Ouyang Z, Tan Y, Wu H, Liu Y. Activating macrophages for enhanced osteogenic and bactericidal performance by Cu ion release from micro/nano-topographical coating on a titanium substrate. *Acta Biomater.* 2019;100:415–426. doi:10.1016/j.actbio.2019.09.030
- Sedelnikova MB, Komarova EG, Sharkeev YP, et al. Modification of titanium surface via Ag-, Sr- and Si-containing micro-arc calcium phosphate coating. *Bioact Mater.* 2019;4:224–235. doi:10.1016/j.bioactmat.2019.07.001
- Zhang R, Xu N, Liu X, et al. Micro/nanostructured TiO<sub>2</sub>/ZnO coating enhances osteogenic activity of SaOS-2 cells. *Artif Cells Nanomed Biotechnol.* 2019;47(1):2838–2845. doi:10.1080/21691401.2018.1546187
- Zhou J, Wang X, Zhao L. Antibacterial, angiogenic, and osteogenic activities of Ca, P, Co, F, and Sr compound doped titania coatings with different Sr content. *Sci Rep.* 2019;9(1):14203. doi:10.1038/s41598-019-50496-3
- Nabiyouni M, Bruckner T, Zhou H, Gbureck U, Bhaduri SB. Magnesium-based bioceramics in orthopedic applications. *Acta Biomater.* 2018;66:23–43. doi:10.1016/j.actbio.2017.11.033
- Yoshizawa S, Brown A, Barchowsky A, Sfeir C. Role of magnesium ions on osteogenic response in bone marrow stromal cells. *Connect Tissue Res.* 2014;55(Suppl 1):155–159. doi:10.3109/03008207.2014.923877
- Szesz EM, de Souza GB, de Lima GG, da Silva BA, Kuromoto NK, Lepiński CM. Improved tribo-mechanical behavior of CaP-containing TiO<sub>2</sub> layers produced on titanium by shot blasting and micro-arc oxidation. *J Mater Sci Mater Med.* 2014;25(10):2265–2275. doi:10.1007/s10856-014-5238-9
- Zhu C, Lv Y, Qian C, et al. Proliferation and osteogenic differentiation of rat BMSCs on a novel Ti/SiC metal matrix nanocomposite modified by friction stir processing. *Sci Rep.* 2016;6(1):38875. doi:10.1038/srep38875
- Huang Q, Li X, Elkhooly TA, et al. The Cu-containing TiO<sub>2</sub> coatings with modulatory effects on macrophage polarization and bactericidal capacity prepared by micro-arc oxidation on titanium substrates. *Colloids Surf B Biointerfaces.* 2018;170:242–250. doi:10.1016/j.colsurfb.2018.06.020
- Ehrenfest DMD, Coelho PG, Kang BS, Sul YT, Albrektsson T. Classification of osseointegrated implant surfaces: materials, chemistry and topography. *Trends Biotechnol.* 2010;28(4):198–206. doi:10.1016/j.tibtech.2009.12.003
- Kournetas N, Spintzyk S, Schweizer E, et al. Comparative evaluation of topographical data of dental implant surfaces applying optical interferometry and scanning electron microscopy. *Dent Mater.* 2017;33(8):e317–e327. doi:10.1016/j.dental.2017.04.020
- Fedorovich NE, Alblas J, Hennink WE, Oner FC, Dhert WJ. Organ printing: the future of bone regeneration? *Trends Biotechnol.* 2011;29(12):601–606. doi:10.1016/j.tibtech.2011.07.001
- Gittens RA, McLachlan T, Olivares-Navarrete R, et al. The effects of combined micron/submicron-scale surface roughness and nanoscale features on cell proliferation and differentiation. *Biomaterials.* 2011;32(13):3395–3403. doi:10.1016/j.biomaterials.2011.01.029
- Radha R, Sreekanth D. Insight of magnesium alloys and composites for orthopedic implant applications – a review. *J Magnes Alloys.* 2017;5(3):286–312. doi:10.1016/j.jma.2017.08.003
- Cho LR, Kim DG, Kim JH, Byon ES, Jeong YS, Park CJ. Bone response of Mg ion-implanted clinical implants with the plasma source ion implantation method. *Clin Oral Implants Res.* 2010;21(8):848–856. doi:10.1111/j.1600-0501.2009.01862.x
- Park JW, Kim YJ, Jang JH, Song H. Osteoblast response to magnesium ion-incorporated nanoporous titanium oxide surfaces. *Clin Oral Implants Res.* 2010;21(11):1278–1287. doi:10.1111/j.1600-0501.2010.01944.x
- Rokosz K, Hryniewicz T, Gaiaschi S, et al. Novel porous phosphorus-calcium-magnesium coatings on titanium with copper or zinc obtained by dc plasma electrolytic oxidation: fabrication and characterization. *Materials (Basel).* 2018;11(9):E1680. doi:10.3390/ma11091680
- Yoshizawa S, Brown A, Barchowsky A, Sfeir C. Magnesium ion stimulation of bone marrow stromal cells enhances osteogenic activity, simulating the effect of magnesium alloy degradation. *Acta Biomater.* 2014;10(6):2834–2842. doi:10.1016/j.actbio.2014.02.002
- Lin S, Yang G, Jiang F, et al. A magnesium-enriched 3D culture system that mimics the bone development microenvironment for vascularized bone regeneration. *Adv Sci.* 2019;6(12):1900209. doi:10.1002/advs.201900209
- Li H, Pan H, Ning C, Tan G, Liao J, Ni G. Magnesium with micro-arc oxidation coating and polymeric membrane: an in vitro study on microenvironment. *J Mater Sci Mater Med.* 2015;26(3):147. doi:10.1007/s10856-015-5428-0
- Ma WH, Liu YJ, Wang W, Zhang YZ. Improved biological performance of magnesium by micro-arc oxidation. *Braz J Med Biol Res.* 2015;48(3):214–225. doi:10.1590/1414-431x20144171
- Komori T. Regulation of osteoblast differentiation by Runx2. *Adv Exp Med Biol.* 2010;658:43–49.
- Liu TM, Lee EH. Transcriptional regulatory cascades in Runx2-dependent bone development. *Tissue Eng Part B Rev.* 2013;19(3):254–263. doi:10.1089/ten.teb.2012.0527
- Zhang X, Chen Q, Mao X. Magnesium enhances osteogenesis of BMSCs by tuning osteoimmunomodulation. *Biomed Res Int.* 2019;2019:7908205. doi:10.1155/2019/7908205
- Huang Y, Jin X, Zhang X, et al. In vitro and in vivo evaluation of akermanite bioceramics for bone regeneration. *Biomaterials.* 2009;30(28):5041–5048. doi:10.1016/j.biomaterials.2009.05.077

**International Journal of Nanomedicine**

Dovepress

**Publish your work in this journal**

The International Journal of Nanomedicine is an international, peer-reviewed journal focusing on the application of nanotechnology in diagnostics, therapeutics, and drug delivery systems throughout the biomedical field. This journal is indexed on PubMed Central, MedLine, CAS, SciSearch<sup>®</sup>, Current Contents<sup>®</sup>/Clinical Medicine,

Journal Citation Reports/Science Edition, EMBase, Scopus and the Elsevier Bibliographic databases. The manuscript management system is completely online and includes a very quick and fair peer-review system, which is all easy to use. Visit <http://www.dovepress.com/testimonials.php> to read real quotes from published authors.

Submit your manuscript here: <https://www.dovepress.com/international-journal-of-nanomedicine-journal>